Cement and Concrete Research 39 (2009) 733–739

Contents lists available at ScienceDirect

Cement and Concrete Research

journal homepage: http://ees.elsevier.com/CEMCON/default.asp

The density of cement phases

M. Balonis [*], F.P. Glasser

Department of Chemistry, Meston Building, University of Aberdeen, Aberdeen, AB24 3UE, Scotland, UK

ARTICLE INFO

Article history:
Received 28 March 2009
Accepted 3 June 2009

Keywords:
Density
X-ray diffraction
Cement
Crystal structure
Characterization

ABSTRACT

The densities of principal crystalline phases occurring in Portland cement are critically assessed and tabulated, in some cases with addition of new data. A reliable and self-consistent density set for crystalline phases was obtained by calculating densities from crystallographic data and unit cell contents. Independent laboratory work was undertaken to synthesize major AFm and AFt cement phases, determine their unit cell parameters and compare the results with those recorded in the literature. Parameters were refined from powder diffraction patterns using CELREF 2 software.

A density value is presented for each phase, showing literature sources, in some cases describing limitations on the data, and the weighting attached to numerical values where an averaging process was used for accepted data. A brief discussion is made of the consequences of the packing of water to density changes in AFm and AFt structures.

Contents

1. Introduction

The densities of cement phases are fundamental parameter with many uses, for example, calculating space filling in pastes by solid cement substances as well as assessment of the potential for changes in dimension and porosity within hardened pastes undergoing phase changes. Yet it is difficult to access a self-consistent set of density data and values reported in the literature for the same substance can vary widely. The importance of having a self-consistent data set has long been recognized: for example Taylor [1] provided data for crystalline calcium silicate hydrates and, in a later publication, gave density and powder diffraction data for many of the main cement phases [2]. Richardson [3] published updated table of crystal data together with density values for calcium silicate hydrates and related phases, but previous compilations regarding other cement compounds are incomplete and somewhat out of date.

The substances comprising cement can be divided into two groups: crystalline and amorphous. The distinction is operational: in the present context, "crystalline" refers to substances having sufficiently regular internal structures, in terms of atomic, ionic and molecular arrangement, to enable characterization by classical crystallographic methods.

---

[*] Corresponding author.
E-mail address: m.balonis@abdn.ac.uk (M. Balonis).

0008-8846/$ – see front matter © 2009 Elsevier Ltd. All rights reserved.
doi:10.1016/j.cemconres.2009.06.005

Some of the relevant phases occur in nature and some can be obtained as single crystals, natural or synthetic. Classical methods of density measurement can often be applied to single crystals. But many cement substances, although crystalline, do not occur in adequate purity or size to apply classical methods. Therefore for most crystalline substances we rely on crystallochemical data for the calculation of densities, but with the cautions given below.

The principal amorphous substance of Portland cement is C–S–H. It presents particular problems in determining its density as it is insufficiently crystalline for application of conventional crystallographic methods: only experimentally-determined measurements are useful. Moreover uncertainties persist especially with respect to its water content and we note that only arbitrary distinctions between "bound" and "free" water are possible. Other phases may also be intercalated within C–S–H on a nanoscale e.g., portlandite or AFm, thus affecting density. Uncertainty therefore exists over the Ca/Si ratio as well as extent of incorporation of other ions (alkali, alumina, sulfate…), all of which potentially affect the density. Finally, possible errors may arise from classical density measurements where, for example, a liquid used for density measurement by the Archimedes method may react with C–S–H. Thus for C–S–H we have no choice but to accept experimentally-determined data.

Crystalline solids, on the other hand, are amenable to calculation of density from crystallographic constants using the relationship:

$$D = (Z \times M) / (N_A \times V)$$

where: D = density in kg/m^3, Z = number of formula units per unit cell, M = formula weight, V the unit cell volume and N_A = Avogadro's number.

Volumes of the unit cells were calculated for relevant crystal systems using standard formulae:

Isometric/cubic crystal system: $V = a^3$
Tetragonal crystal system: $V = a^2c$
Hexagonal/trigonal crystal system: $V = a^2c \sin(60°)$
Orthorhombic crystal system: $V = abc$
Monoclinic crystal system: $V = abc \sin(\beta)$
Triclinic crystal system: $V = abc\,((1 - \cos^2\alpha - \cos^2\beta - \cos^2\gamma) + 2(\cos(\alpha)\cos(\beta)\cos(\gamma))^{1/2}$

where a, b, c are the unit cell axial dimensions and α, β, γ are the relevant angles. In some cases the unit cell contents require elucidation in order to establish the exact chemistry.

The crystallographic approach provides a uniform and consistent basis for calculation but many substances contain defects which result in real densities being slightly lower than calculated (usually the error is less than one part in 10^4) The occurrence of solid solution, in which for example substitution of Fe for Al occurs, also affects the mean atomic mass of ions occupying a particular lattice site or sites and hence the density. Many substances occur in several polytypes, each of which may differ in true unit cell size and symmetry and the possibility exists that preparations may contain mixtures of polytypes. Except where noted, isomorphic substitution is negligible in the selected data. We address polytypism by choosing a single subcell for the calculation and believe that this leads to the correct density, provided the subcell and Z are correctly matched. We also note that rhombohedral crystals have generally been treated on the basis of a larger hexagonal cell: again, no error results provided Z is chosen correctly.

Variable site occupancy may occur, with some sites left partially vacant. For example the subcell water (H_2O) content of ettringite attains a maximum of 36 but more commonly water contents lie in the range 30 to 32H_2O per formula unit, but with little change in cell size occurring in this range. This uncertainty over composition is addressed by stating the formula used for calculation although we also develop density–composition relationships in selected cases. Where a particular phase is impurity-stabilized, the impurity is deemed to be minor but, although the presence of impurity is noted, we are often unable to include it in the formula because no analysis of the phase was recorded in the data source.

Temperature and pressure affect densities and the values shown here are nominally reported for 20°–25 °C and ambient pressure, unless otherwise noted. The literature is often indefinite about the temperature used for collection of crystallographic data apart from stating that data were collected at "room temperature" We have assumed that "room temperature" lies within the range 20–25 °C and have not otherwise attempted corrections.

Where cell dimensions were determined from single crystal methods by the Weissenberg method [19,87], or from precession methods using photographic recording, cell dimensions thus obtained are probably only accurate to ±1%. Therefore where a choice of methods for determination of cell parameters occurred, priority has been given to those made using calibrated powder X-ray diffraction or automated single-crystal methods with electronic recording.

For syngenite, the values given in [40,41] are preferred because the coefficients of thermal dilation, necessary to correct data obtained at 154 K [39] to ambient are not available.

In a few cases our recalculation of density does not agree with the author's own calculation. Where such disagreement exceeds the normal limits of arithmetic error, author's values are noted (Table 1), but we have generally been unable to resolve the discrepancy between calculations.

This work is not complete because of multiplicity of phases, hydration states, and solid solution possibilities but it does include most of the significant compounds occurring in Portland cement and cement pastes. The order of data presentation divides substances into twelve main groups:

- Simple oxides and hydrated oxides
- Carbonates
- Sulfates and hydrated sulfates
- Tricalcium aluminate
- Tetracalcium aluminoferrite
- Tricalcium silicate
- Dicalcium silicate
- Aluminate-ferrite-trisubstituent phases
- Aluminate-ferrite-monosubstituent phases
- Hydrogarnet
- Selected crystalline calcium silicate hydrates structurally related to C–S–H (data including other calcium silicate hydrates presented by Richardson [3])
- Hydrotalcite and related phases.

Experimental work was also undertaken to synthesize major AFm and AFt cement phases, determine their unit cell parameters and compare the results with those recorded in the literature. The preparative routes are described because of great interest amongst the cement community in accessing recipes. Results obtained from these preparations are included in the compilation.

2. Synthesis and characterization of AFm and AFt phases

Many of these preparation routes are described in the previous literature and were used here with minor changes. The synthesis of

Table 1
Density of selected cement phases given by some authors, where our recalculation of density does not agree with the author's own calculation.

Author/reference	Formula	Density given by author [kg/m^3]
Gaines, et al. [9]	SiO_2	2660
Abriel [32]	$CaSO_4 \cdot 0.8H_2O$	2630
Okada, et al. [38]	$K_3\,Na(SO_4)_2$	2690
Swanson, et al. [60]	$[Ca_3Al(OH)_6]_2(SO_4)_3 \cdot (24+2)H_2O$	1754
Rinaldi, et al. [73]	$Ca_2Al_2SiO_7 \cdot 8H_2O$	1960
Rinaldi, et al. [84]	$Ca_3Al_2\,SiO_4(OH)_8$	2760

the relevant cement hydrates required several solid precursors. These were made from analytical reagent grade (AR) chemicals. Lime, CaO, was obtained by decarbonation of AR grade $CaCO_3$ at 1000 °C for ~24 h. Anhydrite, $CaSO_4$, was prepared by dehydration of AR gypsum ($CaSO_4 \cdot 2H_2O$) in a muffle furnace at 550 °C for 12 h.

Tricalcium aluminate, C_3A ($Ca_3Al_2O_6$), was prepared from a 3:1 molar ratio of $CaCO_3$ and Al_2O_3, fired in a platinum crucible at 1400 °C for 3 days in an electrically heated furnace. Every 12 h, the sample was cooled, reground in an agate mortar to achieve homogenization, placed back in the platinum crucible and reheated, repeating until free lime was no longer present.

2.1. AFm phases

Using the above precursors, "hydroxy-AFm", $Ca_4Al_2(OH)_{14} \cdot 6–12H_2O$, was synthesized by mixing CaO and C3A in a 1:1 molar ratio. The solids were slurried in degassed, ultra pure CO_2-free water (water/solid ratio ~10) and reacted at 5 °C in a sealed system with stirring for the first 72 h and thereafter periodically agitated at 5 °C for 3 weeks. Finally the solid was vacuum filtered at 5 °C under N_2 atmosphere. The water state, determined by thermogravimetry, is described subsequently.

2.1.1. Monosulfoaluminate

"Monosulfoaluminate", $Ca_4Al_2(SO_4)(OH)_{12} \cdot 6H_2O$, becomes more stable at temperatures above 40 °C, therefore a 1:1 molar mixture of C_3A and $CaSO_4$ was suspended in ultra pure, CO_2-free water (water/solid ratio ~10), and reacted at 85 °C. After 7 days the solid was vacuum filtered under N_2 atmosphere.

2.1.2. Monocarboaluminate

"Monocarboaluminate", $Ca_4Al_2(CO_3)(OH)_{12} \cdot 5H_2O$, was prepared by mixing C_3A and $CaCO_3$ in a 1:1 molar ratio with previously degassed ultra-pure water at 25 °C and stored for 10 days with periodic agitation.

2.1.3. Hemicarboaluminate

"Hemicarboaluminate", $Ca_4Al_2(CO_3)_{0.5}(OH)_{13} \cdot 5.5H_2O$, was made by addition of C_3A, $CaCO_3$ and CaO in stoichiometric quantities to previously degassed ultra pure water at 25 °C at a w/s ratio about 10 and continuously stirred in plastic (HDPE) bottles for 14 days before filtration.

2.1.4. Strätlingite

Strätlingite, $Ca_2Al_2SiO_2(OH)_{10} \cdot 3H_2O$, was synthesized from a stoichiometric mix of CaO, $Na_2Si_2O_5 \cdot 2H_2O$, $NaAlO_2$ and water at 25 °C. The water:solid ratio was ~10. The suspension was stirred for 5–6 weeks at 25 °C. After filtration, sodium was washed out by flushing the remaining solid with double distilled water. From previous experience the sodium content of the washed solid is known to be negligible.

2.1.5. Friedel's salt

'Friedel's salt' $Ca_4Al_2(Cl)_2(OH)_{12} \cdot 4H_2O$ was made by mixing C_3A and $CaCl_2 \cdot 2H_2O$ in a 1:1 molar ratio, which were dispersed in double distilled, CO_2 free water (w/s~10), sealed in an airtight polythene bottle and left to age with stirring for 30 days. After ageing the solid was filtered under nitrogen atmosphere.

2.2. AFt phases

To prepare 'sulfate ettringite', $Ca_6Al_2(SO_4)_3(OH)_{12} \cdot 26H_2O$, two reactant solutions were initially made, solution (1) by adding 6.65 g $Al_2(SO_4)_3$ $18H_2O$ to 100 ml and solution (2) by dispersing 4.44 g $Ca(OH)_2$ in 250 ml of ultra pure water (>14 MΩ cm) all under CO_2-free conditions. The two reactant solutions were transferred to a N_2-filled glove box, mixed and diluted to 500 ml with additional reagent water to which 0.5 ml of 1 M NaOH had been added. The preparation was sealed in a 500 ml high density polyethylene (HDPE) bottle, removed form the dry box and placed on a hot plate at 60 °C, with stirring. After 48 h, the contents were filtered under N_2 using a ceramic filter funnel and rapidly dried under N2 using a poor vacuum.

'Carbonate ettringite', $Ca_6Al_2(CO_3)_3(OH)_{12} \cdot 26H_2O$, was prepared by precipitation from a stochiometric mixture of CaO, $NaAlO_2$ and Na_2CO_3 in a 10% w/v sucrose solution. Previously-prepared slurries of sodium aluminate and sodium carbonate were added to the sucrose–portlandite mixture, stirred for 3 days and periodically agitated at 25 °C for 2 weeks and thereafter filtered and washed. Experience of this preparation indicated that thorough washing was required to prevent retention of sucrose. The purified product needs analysis to ensure it sucrose-free.

2.3. Data collection

A Bruker D8 advance powder diffractometer was used for characterization and X-ray analysis. Data were collected using Cu Kα radiation at room temperature (25 °C): the angular range was set between 5 and 55° 2θ. Unit cell parameters were refined from the powder diffraction patterns using CELREF 2 software.

The number of selected reflections admitted into the unit cell refinement is shown below:

$Ca_4Al_2(OH)_{14} \cdot 13H_2O$ — 22 reflections
$Ca_4Al_2(SO_4)(OH)_{12} \cdot 6H_2O$ — 23 reflections
$Ca_4Al_2(CO_3)(OH)_{12} \cdot 5H_2O$ — 27 reflections
$Ca_2Al_2SiO_2(OH)_{10} \cdot 3H_2O$ — 29 reflections
$Ca_4Al_2(CO_3)_{0.5}(OH)_{13} \cdot 5.5H_2O$ — 22 reflections
$Ca_4Al_2(Cl)_2(OH)_{12} \cdot 4H_2O$ — 23 reflections
$Ca_6Al_2(SO_4)_3(OH)_{12} \cdot 26H_2O$ — 71 reflections
$Ca_6Al_2(SO_4)_3(OH)_{12} \cdot 30H_2O$ — 38 reflections
$Ca_6Al_2(CO_3)_3(OH)_{12} \cdot 26H_2O$ — 35 reflections.

3. Results

A summary of recommended values is provided in Table 2.

4. Discussion

The classification of cement phases as 'important' (and hence worthy of inclusion) is partly a matter of opinion and partly a matter of the availability of data. For example data on solid solutions at well-spaced intervals are largely absent.

The compilation therefore rests on the values critically extracted from the literature but with a special focus on AFm and AFt phases. Where multiple data were available, and admitted into the compilation, an averaging process was used and density described as 'mean density'. If some methods had relatively poor absolute accuracy [19,39,87] and data were rejected or not heavily weighted, the density is expressed as 'recommended density'. For brevity, only the compiled values are given here with selected key references. A worksheet was generated for each substance showing all references and numerical values, together with comment: the worksheets are accessible on the Nanocem website: http://www.nanocem.org/fileadmin/nanocem_files/documents/MC-RTN/Projects/Project_1/The_densitiy_of_cement_phases_worksheets.pdf.

Review shows that quality of data reported in the literature varies. One of the principal difficulties of determining the densities of substances experimentally by classical methods is in providing assurance that preparation is phase-pure. This assurance is often given by using single crystals, or handpicking enough smaller crystals, for analysis. With cement phases, this is often not possible: not only are crystals too small to select, but an ever-present inaccuracy arises because

Table 2
Density of selected cement phases at 20–25 °C, t.w. — this work.

Mineral or chemical name	Formula	Density [kg/m^3]	References
Lime	CaO	3341	[4,5]
Periclase	MgO	3584	[5,6]
Corundum	Al_2O_3	3990	[5,7,8]
Quartz	SiO_2	2641	[9,10]
Gibbsite	$Al(OH)_3$	2421	[11,12]
Brucite	$Mg(OH)_2$	2368	[13,14]
Portlandite	$Ca(OH)_2$	2251	[15,16]
Calcite	$CaCO_3$	2710	[17–19]
Aragonite	$CaCO_3$	2930	[20,21]
Vaterite	μ-$CaCO_3$	2661	[22,23]
Magnesite	$MgCO_3$	3011	[18,24]
Dolomite	$CaMg(CO_3)_2$	2852	[18,25–27]
Anhydrite	$CaSO_4$	2968	[28–30]
'Soluble anhydrite'	$Ca(SO_4)\cdot <0.05H_2O$	2958	[31]
Hemihydrate	$CaSO_4\cdot 0.5H_2O$	2733	[31]
Hemihydrate	$CaSO_4\cdot 0.8H_2O$	2783	[32]
Gypsum	$CaSO_4\cdot 2H_2O$	2311	[33,34]
Arcanite	K_2SO_4	2668	[35]
Thenardite	Na_2SO_4	2662	[36,37]
Aphthitalite	$K_3\ Na(SO_4)_2$	2703	[38]
Syngenite	$K_2Ca(SO_4)_2\cdot H_2O$	2575	[39–41]
'Aluminosulfate'	$Ca_4(Al_2O_3)_3(SO_4)$	2607	[42]
'Silicosulfate'	$Ca_5(SiO_2)_2(SO_4)$	2972	[43]
Tricalcium aluminate (cubic)	$Ca_3Al_2O_6$	3030	[44–46]
Tricalcium aluminate (othorombic)	$Ca_3Al_2O_6$	3023	[46]
Tetracalcium aluminoferrite	$Ca_2(Al,Fe)_2O_5$	3708	[47,48]
R-tricalcium silicate at 1200 °C	R-Ca_3SiO_5	3025	[49]
R-tricalcium silicate-Sr stabilized	R-Ca_3SiO_5	3168	[50]
M3-tricalcium silicate-Mg stabilized	M3-Ca_3SiO_5	3182	[51]
M3-tricalcium silicate-less well ordered	M3-Ca_3SiO_5	3153	[52]
T1-tricalcium silicate	T1-Ca_3SiO_5	3120	[53]
α-dicalcium silicate-Ba stabilized	α-Ca_2SiO_4	2968	[54]
α'_H-dicalcium silicate-P_2O_5 stabilized	α'_H-Ca_2SiO_4	3148	[55]
α'_L-dicalcium silicate-Sr stabilized	α'_L-Ca_2SiO_4	3092	[50]
β-dicalcium silicate	β-Ca_2SiO_4	3326	[56,57]
γ-dicalcium silicate	γ-Ca_2SiO_4	2960	[58]
Ettringite with low H_2O content ($30H_2O$)	$[Ca_3Al(OH)_6]_2(SO_4)_3\cdot 24H_2O$	1768	[61]
Ettringite ($32H_2O$)	$[Ca_3Al(OH)_6]_2(SO_4)_3\cdot(24+2)H_2O$	1778	[59–62, t.w.]
Ettringite with high H_2O content ($36H_2O$)	$[Ca_3Al(OH)_6]_2(SO_4)_3\cdot(24+6)H_2O$	1863	[61, t.w.]
Carbonate ettringite	$[Ca_3Al(OH)_6]_2(CO_3)_3\cdot(24+2)H_2O$	1760	[59, t.w.]
Iron ettringite	$[Ca_3Fe(OH)_6]_2(SO_4)_3\cdot(24+2)H_2O$	1830	[59,63]
Thaumasite	$Ca_3(SO_4)(CO_3)[Si(OH)_6]\cdot 12H_2O$	1882	[64,65]
Hydroxy-AFm	$Ca_4Al_2(OH)_{14}\cdot 6H_2O$	2044	[66, t.w.]
Fe-hydroxy AFm	$Ca_4Fe_2(OH)_{14}\cdot 6H_2O$	2162	[67]
α1-tetracalcium aluminate-19-hydrate	α1-$Ca_4Al_2(OH)_{14}\cdot 12H_2O$	1804	[68]
α2-tetracalcium aluminate-19-hydrate	α2-$Ca_4Al_2(OH)_{14}\cdot 12H_2O$	1802	[68]
Monosulfoaluminate ($12H_2O$)	$Ca_4Al_2(SO_4)(OH)_{12}\cdot 6H_2O$	2015	[61,69,70, t.w.]
Monosulfoaluminate ($14H_2O$)	$Ca_4Al_2(SO_4)(OH)_{12}\cdot 8H_2O$	1998	[61]
Monosulfoaluminate ($16H_2O$)	$Ca_4Al_2(SO_4)(OH)_{12}\cdot 10H_2O$	1983	[61]
Fe-monosulfoaluminate	$Ca_4Fe_2(SO_4)(OH)_{12}\cdot 6H_2O$	2117	[71,72]
Strätlingite	$Ca_2Al_2SiO_7\cdot 8H_2O$	1937	[73–75, t.w.]
Monocarboaluminate	$Ca_4Al_2(CO_3)(OH)_{12}\cdot 5H_2O$	2175	[66,76, t.w.]
Fe-monocarboaluminate	$Ca_4Fe_2(CO_3)(OH)_{12}\cdot 6H_2O$	2219	[77]
Hemicarboaluminate	$Ca_4Al_2(CO_3)_{0.5}(OH)_{13}\cdot 5.5H_2O$	1985	[66, t.w.]
Dicalcium aluminate-8-hydrate	$Ca_2Al_2(OH)_{10}\cdot 3H_2O$	1950	[78]
α-Friedel's salt	α-$Ca_4Al_2(Cl)_2(OH)_{12}\cdot 4H_2O$	2064	[79–81, t.w.]
β-Friedel's salt	β-$Ca_4Al_2(Cl)_2(OH)_{12}\cdot 4H_2O$	2094	[71,79,81,82]
β-Fe-Friedel's salt	β-$Ca_4Fe_2(Cl)_2(OH)_{12}\cdot 4H_2O$	2228	[71,83]
Kuzel's salt	$Ca_4Al_2(SO_4)_{0.5}(Cl)(OH)_{12}\cdot 6H_2O$	2114	[71,77]
Fe-Kuzel's salt	$Ca_4Fe_2(SO_4)_{0.5}(Cl)(OH)_{12}\cdot 6H_2O$	2222	[71]
Hydrogarnet (katoite)	$Ca_3Al_2(OH)_{12}$	2530	[84–86]
Fe-hydrogarnet	$Ca_3Fe_2(OH)_{12}$	2809	[2,87]
Siliceous hydrogarnet	$Ca_3Al_2\ SiO_4(OH)_8$	2832	[87,88]
Jennite	$9CaO\cdot 6SiO_2\cdot 11H_2O$	2331	[2,89,90]
Tobermorite 14 Å	$5CaO\cdot 6SiO_2\cdot 8H_2O$	2228	[2,91]
Afwillite	$3CaO\cdot 2SiO_2\cdot 3H_2O$	2645	[92,93]
Hydrotalcite	$Mg_4Al_2(OH)_{12}CO_3\cdot 3H_2O$	2122	[94,96]
Fe-hydrotalcite	$Mg_4Fe_2(OH)_{12}CO_3\cdot 3H_2O$	2269	[95]
Meixnerite	$Mg_6Al_2(OH)_{18}\cdot 4H_2O$	1945	[97,98]
OH-hydrotalcite	$Mg_4Al_2(OH)_{14}\cdot 3H_2O$	2036	[98]

bulk preparations may contain significant content of amorphous material which escapes detection by X-ray powder analysis, etc.

Regarding natural samples we have to take into consideration solid solution as well as possible physical inclusions which may affect density. However by determining unit cell sizes, coupled with the known cell contents, errors arising from physical inclusions, adhering impurities, etc. are eliminated: unit cell sizes as determined by refinement of the powder pattern are also insensitive to the presence of non-crystalline impurities.

The use of crystallographic methods also calls into question the definition of a 'phase'. For example, the cement literature tends to treat 'AFm' as though it were a single phase, but we know that this is an oversimplification: recent studies have disclosed that several AFm phases may coexist, which form limited solid solutions. Thus the density classification reflects current knowledge and, as data permit, densities are also given for AFm phases differing in water content e.g. 13 and $19H_2O$ states (hydroxy-AFm), for different trivalent substituents in the principle layer e.g. with octahedral Al or Fe (III) and with different anions, e.g. sulfate, chloride, carbonate and hydroxide. Data are however available for only a few permutations; indeed not all the permutations may be stable and in at least two known examples, phase development is further complicated by ordering of anionic substituents, as occurs in Kuzel's salt (distinguished by ordering of Cl and SO_4) and in hemicarboaluminate (distinguished by ordering of OH and CO_3). It appears that ordered AFm arrangements require both a mono- and divalent anionic substituent and it is possible that other, as yet undiscovered, anion-ordered AFm phases exist.

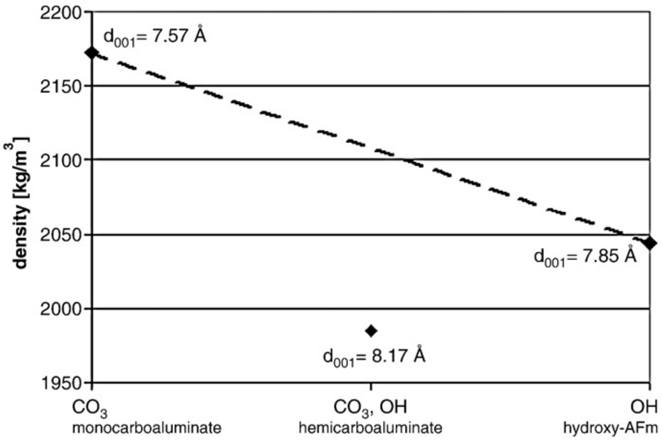

Fig. 1. Density trends in the (OH, CO_3) AFm phases.

Problems of assessing the impact of solid solution on densities have been noted. For example, as expected from the relative formula weights, the density of Al–AFm is much less than the density of corresponding Fe (III)–AFm (Al = 27 g/mol, Fe = 55.8 g/mol). Given that the two AFm phases are isostructural, or very nearly isostructural, the density difference is expected. In the absence of data on intermediate compositions, Vegard's law (that density is a linear function of composition) has to be assumed.

However a number of systems are known in which significant departure from Vegard's law occurs: for example in the Al–AFm series with (OH, SO_4) anions, where solid solution is incomplete but no ordered compound occurs, analysis of the thermodynamic data discloses that sulfate has a strong stabilizing action on the OH–AFm phase [99], i.e., that the solid solutions are non-ideal. It may be that similar non-ideal changes are reflected in the density function.

Other possibilities occur for non-ideal solid solution. For example, carbonate can replace other anions in AFm. While some anions, e.g. chloride and hydroxide appear to behave as simple spherical ions, carbonate can appear either as a spherical ion or as a trigonal planar group. Depending on carbonate orientation, the two possibilities differ in the effective molar volume of the anionic substituent and hence differ in their contribution to density. Fig. 1 shows the densities in the series of AFm phases with OH and CO_3. Of course changing composition influences density but the density of hemi- and monocarboaluminate are also affected by the orientation of the trigonal planar carbonate group. It is most efficiently packed in monocarboaluminate, in which it is sub-parallel to the principal layer spacing [2,100], hence the high density, whereas in hemicarboaluminate, it is perpendicular to the principal layers. Thus the density of hemicarboaluminate falls much below the trend line deduced for its end-members. These differences in carbonate orientation also affect the basal spacings (d_{001}), numerical values of which are shown in Fig. 1.

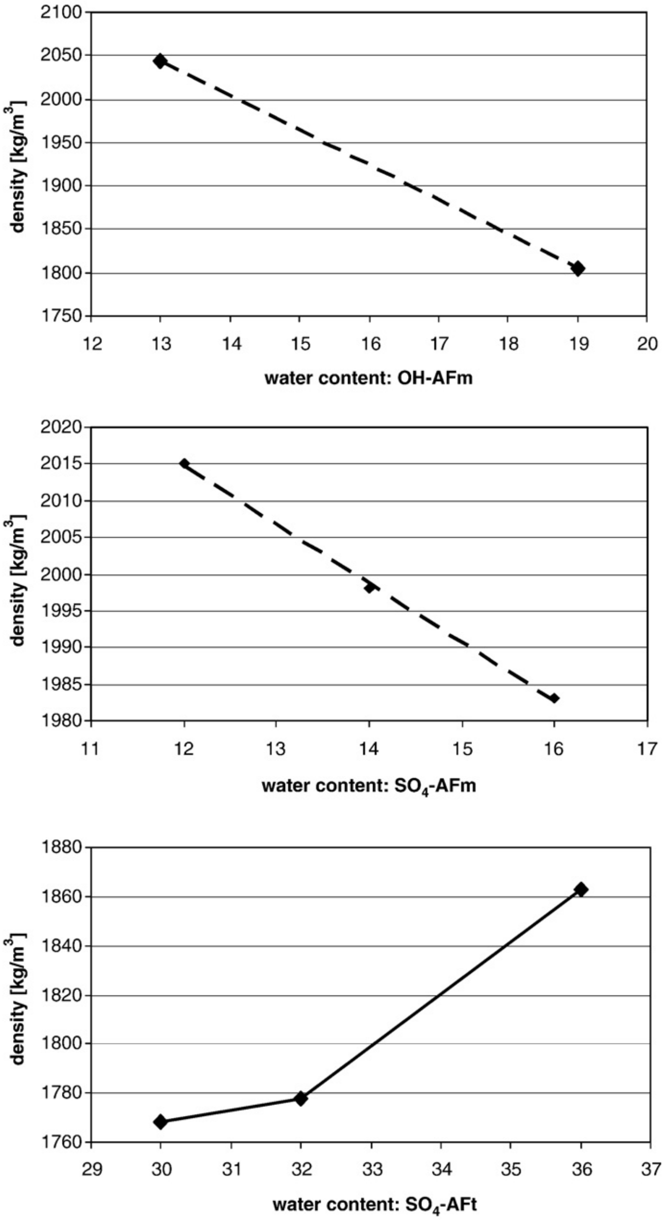

Fig. 2. Relation between water content and density of: OH–AFm (top), SO_4–AFm (middle) and SO_4–AFt (bottom).

Interesting relations exists between the composition and density relationships in the AFm and AFt families, as shown in Fig. 2. The two structures, of AFm and AFt, differ in bonding requirements. The layer spacings in AFm are easily increased to allow variable water contents, as a result of which the density decreases as the water content increases. This relation appears to be linear (as expected) for OH–AFm but it is also observed to be approximately linear for the SO_4–AFm series, where we have three data. The structural role of water is relatively well-defined: we can for example have the $13H_2O$ state or $19H_2O$ state but not, apparently, intermediate water contents, which can only be achieved by having a mixture of discrete AFm phases. For that reason, trend lines are shown as dashed, to emphasize that water contents are not continuously variable within a single AFm phase. Similarly, sulfate AFm at room temperature exhibits three hydrate states: $12H_2O$, $14H_2O$ and $16H_2O$, depending on relative humidity. Pöllmann has established three additional lower hydration states, the densities of which are not sufficiently well established to show in Fig. 2 (middle).

However the three examples of sulfate AFm phases show a linear trend of decreasing density with increasing water content, with a much lower slope than observed for OH–AFm.

The actual hydration state achieved by AFm in cement is not always well known: as we have described, loss of water may occur in the course of specimen preparation unless special precautions are taken in the course of specimen preparation and handling. However it is apparent that large potential volume changes can occur in AFm, should its hydration state change. The greatest potential seems to occur for OH–AFm, where the transition from $13H_2O$ to $19H_2O$ results in an increase in specific volume of more than 10%. For sulfate AFm, a comparable change occurs but is less marked, only a few %. It appears that the more strongly bonded water occupies less effective volume than more weakly bonded, space requirements of which approach that of free water.

The calculated volume change cannot be associated with an actual expansion or contraction: it is best regarded as indicating a *potential for change*. This potential might, for example, be achieved in the course of thermal cycling because, other factors being equal, the highest hydration states are achieved at low temperatures. Nevertheless, the potential for expansion can be minimized by inclusion of sufficient sulfate to convert all AFm to its sulfated form with perhaps a sufficient reserve to stabilize AFt in the cement. Because sufficient sulfate is usually added to Portland cement to achieve this mineralogical state, the problem of dimensional instability resulting from changing AFm hydration states is unlikely to arise in commercial Portland cements. The arguments continue about optimum sulfate content in cement but we note that there are good reasons, more than just control of set times, why cement should not be under-sulfated: in this instance, to avoid potential dimensional instability resulting from the presence of OH–AFm in different hydration states.

The hydration states of AFt show a non-linear density trend in response to changing water content, Fig. 2 (bottom). However the density trend shows a slope opposite to that of AFm: intercalation of more water in the AFt structure *increases* the physical density. This state is believed to arise because AFt is a three dimensional structure; it is not easy to expand or contract its framework so water in excess of

$30H_2O$ per formula unit has to fit into a relatively unchanged physical space. However between 30 and $32H_2O$ the volume change per water molecule changes much less than between 32 and 36. Probably water in excess of 32 occupies a different set of sites than between 30 and 32, thus impacting differently on cell dimensions.

Many reactions occurring in cementitious systems are isochemical: that is, the chemistry remains constant but a redistribution of ions occurs amongst coexisting phases. This compilation might serve as a benchmark to enable the precise calculation of volume changes to be made in the course of isochemical mineralogical changes. Reactions between cement and its service environment generally involve exchange of mass: that is, they are not isochemical. In these conditions, the database presented forms the basis of calculation but requires application of more sophisticated calculations, taking into account the impact of mass balance changes.

Acknowledgments

Magdalena Balonis is grateful to the European Community under the Marie Curie Research Training Network MRTN-CT-2005-019283 "Fundamental understanding of cementitious materials for improved chemical physical and aesthetic performance" (http://www.nanocem.org/MC-RTN/) for the full support of MC project 1.

References

[1] H.F.W. Taylor, Crystallographic Data for the Calcium Silicates, HMSO, London, UK, 1956.

[2] H.F.W. Taylor, Cement Chemistry, 2nd ed, Thomas Telford Publishing, London, UK, 1997.

[3] I.G. Richardson, The calcium silicate hydrates, Cement and Concrete Research 38 (2008) 137–158.

[4] M.C. Morris, H.F. McMurdie, E.H. Evans, B. Paretzkin, J.H. de Groot, R. Newberry, C.R. Hubbard, S.J. Carmel, National Bureau of Standards Monograph 25 (14) (1977) 49.

[5] G. Fiquet, P. Richet, G. Montagnac, High-temperature thermal expansion of lime, periclase, corundum and spinel, Physics and Chemistry of Minerals 27 (1999) 103–111.

[6] R.M. Hazen, Effects of temperature and pressure on the cell dimensions and isotropic temperature factors of periclase, American Mineralogist 61 (1976) 266–271.

[7] H.E. Swanson, E. Tatge, National Bureau of Standards Circular 539 (2) (1953) 20.

[8] E.N. Maslen, V.A. Streltsov, N.R. Streltsova, N. Ishizawa, Y. Satow, Synchrotron X-ray study of the electron density in –Al_2O_3, Acta Crystallographica B49 (1993) 973–980.

[9] R.V. Gaines, H.C.W. Skinner, E.E. Foord, B. Mason, A. Rosenzweig, Dana's New Mineralogy, Eighth Edition, John Wiley & Sons, New York, 1997, pp. 1573–1586.

[10] J. Glinnemann, H.E. King Jr., H. Schulz, T. Hahn, S.J. La Placa, F. Dacol, Crystal structures of the low-temperature quartz-type phases of SiO_2 and GeO_2 at elevated pressure, Zeitschrift für Kristallographie 198 (1992) 177–212.

[11] H. Saalfeld, M. Wedde, Refinement of the structure of gibbsite, $Al(OH)_3$, Zeitschrift für Kristallographie 139 (1974) 129–135.

[12] E. Balan, M. Lazzeri, G. Morin, F. Mauri, First-principles study of the OH-stretching modes of gibbsite, American Mineralogist 91 (2006) 115–119.

[13] H.E. Swanson, N.T. Gilfrich, M.I. Cook, National Bureau of Standards Circular 539 (6) (1956) 62.

[14] L. Desgranges, G. Calvarin, G. Chevrier, Interlayer interactions in $M(OH)_2$: a neutron diffraction study of $Mg(OH)_2$, Acta Crystallographica B52 (1996) 82–86.

[15] L. Desgranges, D. Grebille, G. Calvarin, G. Chevrier, N. Floquet, J.-C. Niepce, Hydrogen thermal motion in calcium hydroxide: $Ca(OH)_2$, Acta Crystallographica B49 (1993) 812–817.

[16] H.E. Swanson, E. Tatge, National Bureau of Standards Circular 539 (1) (1953) 95.

[17] E.N. Maslen, V.A. Streltsov, N.R. Streltsova, X-ray study of the electron density in calcite, $CaCO_3$, Acta Crystallographica B49 (1993) 636–641.

[18] H. Effenberger, K. Mereiter, J. Zemann, Crystal structure refinements of magnesite, calcite, rhodochrosite, siderite, smithsonite, and dolomite, with discussion of some aspects of the stereochemistry of calcite type carbonates, Zeitschrift für Kristallographie 156 (1981) 233–243.

[19] H. Chessin, W.C. Hamilton, B. Post, Position and thermal parameters of oxygen atoms in calcite, Acta Crystallographica 18 (1965) 689–693.

[20] J.P.R. De Villiers, Crystal structures of aragonite, strontianite, and witherite, American Mineralogist 56 (1971) 758–767.

[21] M.C. Morris, H.F. McMurdie, E.H. Evans, B. Paretzkin, J.H. deGroot, R. Newberry, C.R. Hubbard, S.J. Carmel, National Bureau of Standards Monograph 25 (14) (1977) 44.

[22] S.R. Kamhi, On the structure of vaterite $CaCO_3$, Acta Crystallographica 16 (1963) 770–773.

[23] H.J. Meyer, Struktur and Fehlordnung des Vaterits, Zeitschrift für Kristallographie 128 (1969) 183–212.

[24] E.N. Maslen, V.A. Streltsov, N.R. Streltsova, N. Ishizawa, Electron density and optical anisotropy in rhombohedral carbonates. III. Synchrotron X-ray studies of $CaCO_3$, $MgCO_3$ and $MnCO_3$, Acta Crystallographica B51 (1995) 929–939.

[25] R.J. Reeder, W.A. Dollase, Structural variation in the dolomite–ankerite solid-solution series: An X-ray, Mdssbauer, and TEM study, American Mineralogist 74 (1989) 1159–1167.

[26] R.J. Reeder, S.A. Markgraf, High-temperature crystal chemistry of dolomite, American Mineralogist 71 (1986) 795–804.

[27] N.L. Ross, R.I. Reeder, High-pressure structural study of dolomite and ankerite, American Mineralogist 77 (1992) 412–421.

[28] A. Kirfel, Will, Charge density in anhydrite, $CaSO_4$, from X-ray and neutron diffraction measurements, Acta Crystallographica B36 (1980) 2881–2890.

[29] F.C. Hawthorne, R.B. Ferguson, Anhydrous sulphates; II, refinement of the crystal structure of anhydrite, Canadian Mineralogist 13 (1975) 289–297.

[30] R. Hartmann, On the unit cell dimensions and bond lengths of anhydrite, European Journal of Mineralogy 1 (1989) 721–722.

[31] G.A. Lager, T. Armbruster, F.J. Rotella, J.D. Jorgensen, D.G. Hinks, A crystallographic study of the low-temperature dehydration products of gypsum, $CaSO_4.2H_2O$, hemihydrate $CaSO_4 \cdot 0.5H_2O$, and 'γ'-$CaSO_4$, American Mineralogist 69 (1984) 910–918.

[32] W. Abriel, Calcium sulfat subhydrat, $CaSO_4.0,8H_2O$, Acta Crystallographica C39 (1983) 956–958.

[33] B.F. Pedersen, D. Semmingsen, Neutron diffraction refinement of the structure of gypsum, $CaSO_4.2H_2O$, Acta Crystallographica B38 (1982) 1074–1077.

[34] P.F. Schofield, K.S. Knight, I.C. Stretton, Thermal expansion of gypsum investigated by neutron powder diffraction, American Mineralogist 81 (1996) 847–851.

[35] J.A. McGinnety, Redetermination of the structures of potassium sulphate and potassium chromate: the effect of electrostatic crystal forces upon observed bond lengths, Acta Crystallographica B28 (1972) 2845–2852.

[36] B.N. Mehrotra, Th. Hahn, W. Eysel, H. Rtipke, A. Illguth, Crystal chemistry of compounds with thenardite (Na_2SO_4V) structure, Neues Jahrbuch für Mineralogie Monatshefte (1978) 408–421.

[37] F.C. Hawthorne, R.B. Ferguson, Anhydrous sulphates; I, refinement of the crystal structure of celestite with an appendix on the structure of thenardite, Canadian Mineralogist 13 (1975) 181–187.

[38] K. Okada, J. Ossaka, Structures of potassium sodium sulphate and tripotassium sodium disulphate, Acta Crystallographica B36 (1980) 919–921.

[39] G.B. Bokii, N.A. Pal'chik, M.Y. Antipin, The crystal structure of syngenite, Soviet Physics. Crystallography 23 (1978) 141–143.

[40] E. Corazza, C. Sabelli, The crystal structure of syngenite, $K_2Ca(SO_4)_2{}^*(H_2O)$, Zeitschrift fur Kristallographie 124 (1967) 398–408.

[41] E. Aruja, On the unit cell of calcium potassium sulphate hydrate: synthetic and natural syngenite, Mineralogical Magazine 31 (1958) 943–946.

[42] P.E. Halstead, A.E. Moore, The composition and crystallography of an anhydrous calcium aluminosulphate occurring in expanding cement, Journal of Applied Chemistry 12 (1962) 413–417.

[43] P.D. Brotherton, J.M. Epstein, M.W. Pryce, A.H. White, Crystal structure of 'calcium sulphosilicate' $Ca_5(SiO_4)_2SO_4$, Australian Journal of Chemistry 27 (1974) 657–660.

[44] P. Mondal, J.W. Jeffery, The crystal structure of tricalcium aluminate, $Ca_3Al_2O_6$, Acta Crystallographica B31 (1975) 689–697.

[45] H.E. Swanson, Fuyat, G.M. Ugrinic, National Bureau of Standards Circular 539 (5) (1955) 20.

[46] F. Cervantes Lee, F.P. Glasser, Powder diffraction data for compounds in the series $Na_x(Ca_{3\pm x}Na_x)Al_2O_6$, Journal of Applied Crystallography 12 (1979) 407–410.

[47] A.A. Colville, S. Geller, The crystal structure of brownmillerite, Ca_2FeAlO_5, Acta Crystallographica B27 (1971) 2311–2315.

[48] M.C. Morris, H.F. McMurdie, E.H. Evans, B. Paretzkin, J.H. deGroot, C.R. Hubbard, S. J. Carmel, National Bureau of Standards Monograph 25 (16) (1979) 186.

[49] F. Nishi, Y. Takeuchi, The rhombohedral structure of tricalcium silicate at 1200 °C, Zeitschrift für Kristallographie 168 (1984) 197–212.

[50] A.M. Ilyinets, V.I. Simonov, M.Ya. Bikbau, New-data concerning atomic structures of Portland cement silicates, 8th International Congress on the Chemistry of Cement, vol. 6, 1986, pp. 489–491.

[51] F. Nishi, Y. Takeuchi, I. Maki, Tricalcium silicate $Ca_3O[SiO_4]$: the monoclinic superstructure, Zeitschrift für Kristallographie 172 (1985) 297–314.

[52] W.G. Mumme, Crystal structure of tricalcium silicate from a Portland cement clinker and its application to quantitative XRD analysis, Neues Jahrbuch für Mineralogie Monatshefte (1995) 145–160.

[53] N.I. Golovastikov, R.G. Matveeva, N.V. Belov, Crystal structure of tricalcium silicate $CaO \cdot SiO_2$–C_3S, Soviet Physics. Crystallography 20 (1975) 441–445.

[54] S. Udagawa, K. Urabe, T. Iano, Review of the 34th General Meeting, Cement Association of Japan, Tokyo, 1980, p. 37.

[55] H. Saalfeld, X-ray investigation of single crystals of β-Ca_2SiO_4 (larnite) at high temperatures, American Mineralogist 60 (1975) 824–827.

[56] K.H. Jost, B. Ziemer, R. Seydel, Redetermination of the structure of –dicalcium silicate, Acta Crystallographica B33 (1977) 1696–1700.

[57] C.M. Midgley, The crystal structure of –dicalcium silicate, Acta Crystallographica 5 (1952) 307–312.

[58] S. Udagawa, Urabe, M. Natsume, T. Yano, Refinement of the crystal structure of gamma-Ca_2SiO_4, Cement Concrete Research 10 (1980) 139–144.

[59] L.J. Struble, 8th International Congress on the Chemistry of Cement, vol. 6, 1986, pp. 582–588.

[60] H.E. Swanson, N.T. Gilfrich, M.I. Cook, R. Stinchfield, P.C. Parks, National Bureau of Standards Circular 539 (8) (1959) 3.

[61] H. Pöllmann, 'Characterization of Different Water Contents of Ettringite and Kuzelite', proc. XII International Congress on the Chemistry of Cement, 8–13 July 2007, Montreal, Canada, 2009.

[62] H. Pöllmann, S. Auer, H.J. Kuzel, R. Wenda, Solid solution of ettringites. II: incorporation of $B(OH)_4^-$ and CrO_4^{2-} in $3CaO.Al_2O_3.3CaSO_4.32H_2O$, Cement Concrete Research 23 (1993) 422–430.

[63] H.F. McMurdie, M.C. Morris, E.H. Evans, E. Paretzkin, W. Wong-Ng, Y. Zhang, Standard X-ray diffraction powder patterns from the JCPDS research associateship, Powder Diffraction 2 (1) (1987) 41–52.

[64] H. Effenberger, A. Kirfel, G. Will, E. Zobetz, A further refinement of the crystal structure of thaumasite, $Ca_3Si(OH)_6CO_3SO_4\cdot 12H_2O$, Neues Jahrbuch für Mineralogie Monatshefte (1983) 60–68.

[65] S.D. Jacobsen, J.R. Smyth, R.J. Swop, Thermal expansion of hydrated six-coordinate silicon in thaumasite, $Ca_3Si(OH)_6(CO_3)(SO_4)\cdot 12H_2O$, Physics and Chemistry of Minerals 30 (2003) 321–329.

[66] R. Fischer, H.J. Kuzel, Reinvestigation of the system $C_4A\cdot nH_2O–C_4A\cdot CO_2\cdot nH_2O$, Cement Concrete Research 12 (1982) 517–526.

[67] H.E. Schwiete, T. Iwai, Über das Verhalten der ferritischen Phase im Zement während der Hydratation, Zement-Kalk-Gips 17 (1964) 379–386.

[68] E. Aruja, The unit cell and space group of $4CaO\cdot Al_2O_3\cdot 19H_2O$ polymorphs, Acta Crystallographica 14 (1961) 1213–1216.

[69] R. Allmann, Refinement of the hybrid layer structure $[Ca_2Al(OH)_6]^+[1/2(SO_4)\cdot 3H_2O]^-$, Neues Jahrbuch für Mineralogie Monatshefte (1977) 136–144.

[70] H. Pöllmann, T. Witzke, H. Kohler, Kuzelite, American Mineralogist (1998) 909 (abstract).

[71] H.J. Kuzel, Erstaz von Al^{3+} durch Cr^{3+} und Fe^{3+} in $3CaO\cdot Al_2O_3\cdot CaCl_2\cdot nH_2O$ und $3CaO\cdot Al_2O_3\cdot CaSO_4\cdot nH_2O$, Zement-Kalk-Gips 21 (1968) 463–469.

[72] M. Ecker, H.J. Pöllmann, PDF 42-1472, ICDD, Grant in Aid, 1991.

[73] H.J. Kuzel, Crystallographic data and thermal decomposition of synthetic gehlenite hydrate, $2CaO\cdot Al_2O_3\cdot SiO_2\cdot 8H_2O$, Neues Jahrbuch für Mineralogie. Abhandlungen 148 (1976) 319–325.

[74] G. Hentschel, H.J. Kuzel, Strätlingit, $2CaO–Al_2O_3–SiO_2.8H_2O$, ein neues Mineral, Neues Jahrbuch für Mineralogie Monatshefte (1976) 326–330.

[75] R. Rinaldi, M. Sacerdoti, E. Passadlia, Strätlingite: crystal structure, chemistry, and a reexamination of its polytype vertumnite, European Journal of Mineralogy 2 (1990) 841–849.

[76] G. Renaudin, M. Francois, O. Evrard, Order and disorder in the lamellar hydrated tetracalcium monocarboaluminate compound, Cement Concrete Research 29 (1999) 63–69.

[77] G. Simon, Thesis (1984), Erlagen, Germany.

[78] T. Scheller, et al., 6th International Congress on the Chemistry of Cement (Moscow), vol. 2, 1976, p. 217, part 1.

[79] H.J. Kuzel, Röntgenuntersuchung in system $3CaO\cdot Al_2O_3\cdot CaSO_4\cdot nH_2O–3CaO\cdot Al_2O_3\cdot CaCl_2\cdot nH_2O–nH_2O$, Neues Jahrbuch für Mineralogie Monatshefte (1966) 193–200.

[80] A. Terzis, S. Filippakis, H.J. Kuzel, H. Burzlaff, The crystal structure of $Ca_2Al(OH)_6Cl.2H_2O$, Zeitschrift für Kristallographie (1981) 29–34.

[81] J.P. Rapin, G. Renaudin, E. Elkaim, M. Francois, Structual transition of Friedel's salt $3CaO\cdot Al_2O_3\cdot CaCl_2\cdot 10H_2O$ studied by synchrotron powder diffraction, Cement and Concrete Research 32 (2002) 513–519.

[82] G. Renaudin, F. Kubel, J.P. Rivera, M. Francois, Structural phase transition and high temperature phase structure of Friedels salt, $3CaO\cdot Al_2O_3\cdot CaCl_2\cdot 10H_2O$, Cement and Concrete Research 29 (1999) 1937–1942.

[83] F. Götz Neunhoeffer, Ph.D thesis (in german) (1996), University of Erlagen-Nürnberg, Germany, p 124–135.

[84] H.J. Kuzel, Uber die orientierte entwässerung von tricalciumaluminathydrat $3CaOAl_2O_3.\ 6H_2O$, Neues Jahrbuch für Mineralogie Monatshefte (1969) 397–404.

[85] E. Brandenberger, Kristallstrukturelle Untersuchungen an Ca-Aluminathydraten, Schweizerische Mineralogische und Petrographische Mitteilungen 13 (1933) 569 (abstract).

[86] G.A. Lager, T. Armbruster, J. Faber, Neutron and X-ray diffraction study of hydrogarnet $Ca_3Al_2(O_4H_4)_3$, American Mineralogist 72 (1987) 756–765.

[87] E.P. Flint, H.F. McMurdie, L.S. Wells, Hydrothermal and X-ray studies of the garnet–hydrogarnet series and the relationship of the series to hydration products of portland cement, RP 1355, Journal of Research of the National Institute of Standards and Technology U.S. 26 (1941) 13–33.

[88] R. Rinaldi, E. Passaglia, Katoite, a new nember of the $Ca_3Al_2(SiO_4)_3–Ca_3Al_2(OH)_{12}$ series and a new nomenclature for the hydrogrossular group of minerals, Bulletin de Mineralogie 107 (1984) 606–618.

[89] J.A. Gard, H.F.W. Taylor, G. Cliff, G.W. Lorimer, A re-examination of jennite, American Mineralogist 62 (1977) 365–368.

[90] E. Bonaccorsi, S. Merlino, H.F.W. Taylor, The crystal structure of jennite $Ca_9Si_6O_{18}(OH)_6\cdot 8H_2O$, Cement and Concrete Research 34 (2004) 1481–1488.

[91] E. Bonaccorsi, S. Merlino, A.R. Kampf, The crystal structure of Tobermorite 14 Å (Plombierite), a C–S–H phase, Journal of the American Ceramic Society 88 (3) (2005) 505–512.

[92] K.M.A. Malik, J.W. Jeffery, A re-investigation of the structure of afwillite, Acta Crystallographica B32 (1976) 475–480.

[93] H.D. Megaw, The structure of afwillite, $Ca_3(SiO_3OH)_2.2H_2O$, Acta Crystallographica 5 (1952) 477–491.

[94] R. Allmann, H.P. Jepsen, Die struktur des hydrotalkits, Jahrbuch für Mineralogie Monatshefte (1969) 544–551.

[95] T. Sato, H. Fujita, T. Endo, M. Shimada, A. Tsunashima, Synthesis of hydrotalcite-like compounds and their physico-chemical properties, Reactivity of Solids 5 (1988) 219–228.

[96] M. Bellotto, B. Rebours, O. Clause, J. Lynch, D. Bazin, A reexamination of hydrotalcite crystal chemistry, Journal of Physical Chemistry 100 (1996) 8527–8534.

[97] S. Koritnig, P. Süsse, Meixnerite, American Mineralogist 61 (1976) 176 (abstract).

[98] G. Mascolo, O. Marino, A new synthesis and characterization of magnesium–aluminium hydroxides, Mineralogical Magazine 43 (1980) 619–621.

[99] T. Matschei, B. Lothenbach, F.P. Glasser, The AFm phase in Portland cement, Cement and Concrete Research 37 (2007) 118–130.

[100] G. Renaudin, Ph.D thesis (in french) (1998), University of Henri Poincaré, Nancy, France, p 150.